Quantized Vortex Rings in Superfluid Helium*

G. W. RAYFIELD† AND F. REIF
Department of Physics, University of California, Berkeley, California
(Received 10 July 1964)

Evidence is presented to show that charged particles in superfluid helium at low temperatures can be accelerated to create freely moving charge-carrying vortex rings in the liquid. The circulation of these vortex rings can be determined by measuring their energy and velocity; it is found to be equal to one quantum h/m, where h is Planck's constant and m is the mass of a helium atom. The core radius of the vortex is approximately 1 Å. The dynamical properties of such a vortex ring moving under the influence of external forces can be described by a dispersion relation $E \propto p^{1/2}$ connecting its energy E and momentum p; it can also be understood in detail in terms of the hydrodynamic Magnus force. Experiments are described which verify the essential validity of this dynamical analysis. Vortex rings can interact with various quasiparticles in the liquid, i.e., with rotons, phonons, and He^3 impurities. The scattering of these quasiparticles by vortex rings can be investigated by experiments designed to study the temperature dependence of the rate of energy loss of such rings moving through the liquid. In this way it is possible to measure the effective momentum-transfer cross sections for scattering of the various quasiparticles by vortex lines. The cross section thus deduced is 9.5 Å for scattering of rotons and 18.3 Å for scattering of He^3 atoms. The experiments yield only scant information about scattering of phonons, but are not inconsistent with the magnitude of the phonon scattering cross section expected on theoretical grounds.

1. INTRODUCTION

IN earlier work[1,2] ions were used as microscopic probe particles to study the superfluid state of liquid He^4. At temperatures sufficiently below the λ point the liquid can be described in terms of a superfluid ground state and collective excitations (or quasiparticles) of two different types, namely phonons (low momentum excitations) and rotons (high momentum excitations).[3] An ion in the liquid attains thermal equilibrium by collisions with these quasiparticles. In the presence of a sufficiently small electric field $\mathcal{E}$, the energy $e\mathcal{E}l$ gained by an ion in a mean free path l between collisions is much less than its thermal energy kT so that the ion remains essentially in thermal equilibrium. In this case the ion acquires a drift velocity v_D proportional to $\mathcal{E}$. The corresponding mobility $\mu \equiv v_D/\mathcal{E}$ was measured in previous work[1,2] and found to increase exponentially (for $T \gtrsim 0.6°\mathrm{K}$) when the temperature was lowered. These results show that the mean free path l of an ion becomes quite large when the number of thermally excited quasiparticles is reduced. (The estimated magnitude of l is of the order of a micron at 0.5°K). Measurements of this type permitted a detailed investigation of the scattering of an ion by the various excitations of the liquid.

The present work describes investigations in the opposite limit of low temperatures ($0.28° < T < 0.7°\mathrm{K}$) and in the presence of an electric field high enough so that $e\mathcal{E}l \gg kT$. An ion can then acquire sufficient energy between collisions to create excitations in the liquid. Indeed, we have already reported in a previous note[4] (which will henceforth be designated as I) that it is in this way possible to produce in the superfluid charge-carrying quantized vortex rings. The following pages will be devoted to an extensive discussion of investigations dealing with such vortex rings.

In this context it is useful to recall that phonons and rotons are not the only excitations possible in liquid helium. There exist in addition *ma*croscopic excitations involving the flow of large amounts of liquid and hence characterized by considerably higher energy. Suppose that the superfluid at absolute zero is characterized by a stationary rotational flow pattern with flow velocity $\mathbf{v}_s$. In a quantum-mechanical description of the superfluid, this flow pattern can be described by a single well-defined wave function Ψ extending over *ma*croscopic spatial dimensions. One expects this wave function to have the form $\Psi = e^{i\varphi}\Psi_0$, where Ψ_0 is the ground-state wave function of the fluid at rest and where φ is a phase factor whose gradient is related to the flow velocity $\mathbf{v}_s$.[5] The condition that Ψ be single-valued leads then to the requirement that φ change by an integral multiple of 2π in going around any closed path. This requirement is equivalent to the Bohr-Sommerfeld condition in the form

$$\oint \mathbf{p}\cdot d\mathbf{l} = m \oint \mathbf{v}_s \cdot d\mathbf{l} = hN, \qquad (1)$$

where $\mathbf{p}$ is the momentum associated with a helium atom of mass m moving with the flow velocity $\mathbf{v}_s$, h is Planck's

* Work supported in part by the U. S. Office of Naval Research.
† Present address: Department of Physics, University of Pennsylvania, Philadelphia, Pennsylvania.
[1] G. Careri in C. J. Gorter, *Progress in Low Temperature Physics* (Interscience Publishers, Inc., New York, 1961), Vol. 3, pp. 58–79.
[2] F. Reif and L. Meyer, Phys. Rev. **119**, 1164 (1960), and L. Meyer and F. Reif, Phys. Rev. Letters **5**, 1 (1960); also Phys. Rev. **123**, 727 (1961).
[3] K. R. Atkins, *Liquid Helium* (Cambridge University Press, New York, 1959), p. 58; C. T. Lane, *Superfluid Physics* (McGraw-Hill Book Company, Inc., New York, 1962), Chap. 5.
[4] G. W. Rayfield and F. Reif, Phys. Rev. Letters **11**, 305 (1963).
[5] R. P. Feynman in C. J. Gorter, *Progress in Low Temperature Physics* (Interscience Publishers, Inc., New York, 1955), Vol. 1, pp. 34–53.

constant, and N is any integer. The application of quantum mechanics to superfluid helium thus leads to the expectation of quantization on a *macroscopic* scale,[6] the "circulation" κ defined by

$$\kappa \equiv \oint \mathbf{v}_s \cdot d\mathbf{l} \tag{2}$$

being not only constant as it would be classically, but quantized in units of

$$\kappa_0 = h/m = 0.997 \cdot 10^{-3} \text{ cm}^2 \text{ sec}^{-1}. \tag{3}$$

The simplest situation is one of cylindrical symmetry. In this case (2) becomes $\kappa = v_s(2\pi r)$, where r denotes the distance from the symmetry axis and v_s the circumferential component of $\mathbf{v}_s$. Thus

$$v_s = \kappa/2\pi r, \tag{4}$$

a relation characterizing the flow pattern of a vortex line. [Note, however, that if r becomes less than some cutoff parameter a which is called the "core radius," v_s must deviate from the relation (4) since it would otherwise become infinite.[7]] More generally, vortex lines need not be straight. They can be curved and, if they do not terminate on walls, must close on themselves; in particular they can thus form circular vortex rings. But the fundamental quantization condition remains valid.

The existence of quantization on a macroscopic scale is also predicted in the case of superconductors. In that case the momentum $\mathbf{p}$ of an electron pair involves the vector potential so that the condition (1) leads to the quantization of the magnetic flux (or more precisely, the fluxoid) passing through a hollow superconductor. This quantization has recently been confirmed in a set of beautiful experiments.[8] The experimental situation in the case of superfluid liquid helium has been less satisfactory. The only experiment designed to investigate directly the question of macroscopic quantization has been an ingenious arrangement by Vinen[9] in which he attempted to measure the force acting on (and hence the circulation surrounding) a thin wire stretched along the axis of a rotating bucket of superfluid helium. Experimental difficulties were, however, encountered in establishing equilibrium conditions and in avoiding partial attachment of vortex lines to the wire. The measurements led, therefore, to a wide spread in the observed values of κ, although a pronounced maximum was found near the value h/m.

2. EVIDENCE FOR THE CREATION OF QUANTIZED VORTEX RINGS

A. Experiments and Interpretation

In the present experiments a container enclosing the liquid He^4 under investigation and several electrodes could be cooled down to 0.28°K in an apparatus similar to the one described by Reif and Meyer.[10] The apparatus differed predominantly by using a nonrecirculating He^3 refrigerator and a germanium resistance thermometer. Ions were produced in the liquid by α particles from a Po^{210} source immersed in it; ions of either sign could then be drawn out of the source region by appropriate electric fields. The charges arriving at a collecting electrode gave rise to currents (of the order of 10^{-13} A) which could be measured by a Cary vibrating-reed electrometer. Gold-plated grids were used in several different arrangements to control the electric fields between the source and collector (separated by about 2 cm).[11]

The behavior of the charge carriers at some intermediate temperature (like 0.6°K) is very different depending on the strength of the electric field $\mathcal{E}$. If $\mathcal{E}$ is sufficiently small so that $e\mathcal{E}l \ll kT$ (e.g., less than about 1 V/cm), one measures a drift velocity and associated mobility characteristic of charge carriers subject to large frictional effects due to collisions with excitations. On the other hand, if $\mathcal{E}$ is increased sufficiently so that $e\mathcal{E}l \gg kT$ (e.g., $\mathcal{E} \gtrsim 30$ V/cm at 0.6°K), the charge carriers behave like free particles exhibiting inertial properties and subject to relatively small friction. The situation is particularly striking at low temperatures where a very small field is sufficient to satisfy the condition $e\mathcal{E}l \gg kT$. All the experiments described in this section and the following one were carried out at the low temperature of 0.28°K. It is then found that the charge carriers can traverse field-free regions several centimeters in length with negligible loss of energy. They can also move against a retarding field as long as the retarding potential does not exceed the total energy initially imparted to them by the applied electric fields in preceding regions of space.[4] In short, the behavior of a charge carrier can then be simply described (like that of a charged particle in vacuum) by assigning to it a well-defined energy and neglecting frictional effects.

A time-of-flight velocity spectrometer of the type shown in Fig. 1(a) was used to measure the velocity v of these charge carriers as a function of their energy E. If a potential V is applied between the radioactive

[6] L. Onsager, Nuovo Cimento **6**, Suppl. 2, 249 (1949); also R. P. Feynman, Ref. 5.

[7] It is worth pointing out the electromagnetic analogy to a wire of radius a carrying a current I. For an incompressible fluid div $\mathbf{v}=0$ and the vorticity $\mathbf{w} \equiv$ curl $\mathbf{v}=0$ outside the core of the vortex line. For the wire, the magnetic field $\mathbf{H}$ satisfies the Maxwell equations div $\mathbf{H}=0$ and curl $\mathbf{H}=\mathbf{j}$, where $\mathbf{j}$ is the current density which vanishes outside the wire. Hence the field $\mathbf{H}$ surrounding the wire is analogous to the velocity $\mathbf{v}$ about the vortex; and the current $I = \oint \mathbf{H} \cdot d\mathbf{l}$ given by Ampere's law is analogous to the circulation of κ of (1).

[8] B. S. Deaver and W. M. Fairbank, Phys. Rev. Letters **7**, 43 (1961); R. Doll and M. Näbauer, *ibid.* **7**, 51 (1961); W. A. Little and R. D. Parks, *ibid.* **9**, 9 (1962).

[9] W. F. Vinen, Proc. Roy. Soc. (London) **A260**, 218 (1961).

[10] F. Reif and L. Meyer, Phys. Rev. **119**, 1164 (1960).

[11] A more detailed description of the apparatus and the experimental procedures can be found in Appendix III of G. W. Rayfield-thesis, University of California, 1964 (unpublished).

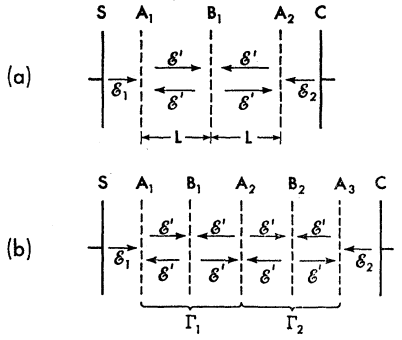

FIG. 1. The time-of-flight velocity spectrometer. The field $\mathcal{E}'$ is reversed ν times per second by applying a square-wave potential to grids B. A single-stage spectrometer is shown in (a), a double-stage spectrometer in (b).

source S and grid A_1, a charge carrier (assumed to be singly charged) arrives at A_1 with an energy $E=$ eV and with some velocity v; it is prevented from reaching the collecting electrode C by a retarding potential ($\approx -V$) applied between A_2 and C. A small square-wave potential of frequency ν is applied to grid B_1 and produces in the region A_1A_2 (free of dc fields) small electric fields $\mathcal{E}'$ alternately directed toward and away from B_1. If v is such that the time of flight L/v of the charge carrier through the distance L from A_1 to B_1 (and thus also from B_1 to A_2) is just equal to the time $(2\nu)^{-1}$ between field reversals, then the carrier remains in synchronism with this field and thus gains from it a small net amount of energy sufficient to overcome the retarding potential between A_2C and to reach the collector C. The current I arriving at C exhibits thus a resonance maximum at the frequency $\nu=\frac{1}{2}(v/L)$ (and at odd harmonics thereof).[12] A measurement of this frequency yields then directly the velocity v of the charge carrier. It is possible to increase the resolution of the method by using two stages of velocity selection in succession, as illustrated in Fig. 1(b) where a square-wave potential of the same frequency ν is applied to both grids B_1 and B_2.

Velocity measurements were thus carried out under varying conditions and with various grid spacings in velocity spectrometers containing either one or two successive stages of velocity selection. The results obtained were reproducible and consistent, but revealed the following two remarkable facts. (a) The measured velocities are very small (e.g., $v=27$ cm/sec when $E=10$ eV), roughly smaller by a factor 10^5 than the calculated velocity in vacuum of a He^4 ion of comparable energy. (b) More striking still, the measured velocity of a charge carrier is found to *de*crease when its energy is *in*creased ($v\propto E^{-1}$ approximately). It was verified that the relation between v and E is unique, i.e., that v depends only on the actual energy E of the charge carrier irrespective of its past history describing how this energy was attained.[4] (Additional details concerning the preceding experiments can be found in I.) The experimental data showing the observed dependence of v on E are summarized in Fig. 2.

The low value of the measured velocity suggests that the charge is strongly coupled to very large amounts of the surrounding liquid so that one observes effectively the motion of a well-defined localized disturbance of the fluid, a disturbance which is essentially macroscopic but labeled by an attached charge. A natural assumption is that this disturbance is a vortex ring which is indeed a hydrodynamically stable entity characterized by an energy E and velocity v approximately related by the proportionality $v\propto E^{-1}$ (reminiscent of that observed for the charge carriers in the present experiments). Figure 3 indicates schematically in cross section the flow pattern of such a vortex ring of radius R. A straight vortex line of circulation κ has associated with it a kinetic energy of rotation E' per unit length. [Here E' is proportional to the integral over space of v_s^2 given by (4), i.e., $E'\propto\kappa^2$.] In first approximation the energy E of the vortex ring is thus given by $E=(2\pi R)E'$ so that $E\propto\kappa^2R$. In order to estimate the axial velocity v of the vortex ring, one can simplify the problem by making it two dimensional, i.e., by replacing the ring in Fig. 3 by a pair of straight vortex lines of opposite circulation separated by a distance $2R$. The flow pattern of one vortex line would not move in space if the other line were absent. But, if the second line is present, it produces at the center of the first line a velocity which is, in accordance with (4), equal to $v=\kappa/(4\pi R)$ and

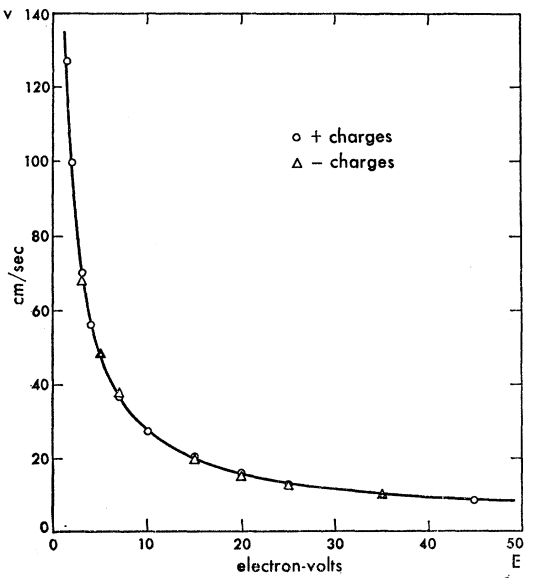

FIG. 2. Relation between the velocity v and energy E of a vortex ring. The points are experimental data for positive and negative charge carriers. The curve is the theoretical relation following from (5) and (6) with $\kappa=h/m$ and $a=1.2$ Å.

[12] The odd harmonics arise because an odd number of field reversals during the time of flight from A_1 to B_1 also results in a small net increment of energy being imparted to the charge carrier.

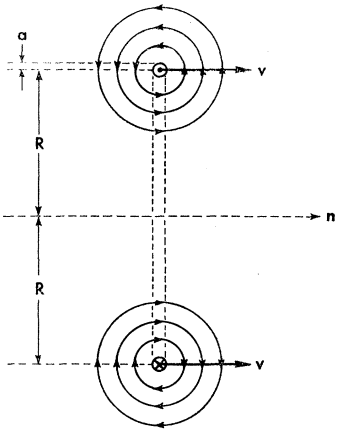

FIG. 3. Schematic illustration showing a vortex ring in cross section. (The actual flow velocity $\mathbf{v}_s$ at any point is a superposition of the flow velocities indicated in the diagram.)

which causes the whole flow pattern of this line to move with this velocity. Similarly, the first line produces at the position of the second line a velocity v of the same direction and magnitude. The net result is that the pair of lines moves under their mutual influence with a velocity $v \propto \kappa/R$. The axial velocity of the vortex *ring* differs only slightly from this result. Hence it follows that a large vortex ring of given circulation κ has a large energy E, but a small velocity v; or somewhat more quantitatively, since $E \propto \kappa^2 R$ while $v \propto \kappa/R$, the ring satisfies the approximate relation $v \propto \kappa^3 E^{-1}$. The presence of an applied force causes then the energy E (and corresponding radius R) of a vortex ring to *in*crease, but as a result its velocity *de*creases.[13] (The dynamical details will be discussed more fully in Sec. 3.)

The exact expressions derived by classical hydrodynamics for the energy and velocity of a vortex ring, moving in an incompressible fluid of density ρ and having a radius R much greater than its core radius a, are[14]

$$E=\tfrac{1}{2}\rho\kappa^2 R[\eta-(7/4)], \tag{5}$$

and

$$v=(\kappa/4\pi R)(\eta-\tfrac{1}{4}), \tag{6}$$

where

$$\eta\equiv\ln(8R/a). \tag{7}$$

Since $R\gg a$, the parameter η is a very insensitive function of R so that the relations (5) and (6) agree to good approximation with the previously mentioned proportionalities $E\propto\kappa^2 R$ and $v\propto\kappa/R$. Note also that (5) and (6) depend on a only logarithmically through η. The behavior of the vortex ring is thus quite insensitive to the exact value of a (expected to be of the order of atomic dimensions) or to specific models describing the behavior of the fluid within this core radius.[15] The question then arises whether the relation between v and E observed for the charge carriers in the present experiments satisfies indeed the functional relation predicted by (5) and (6). If this is the case, one would then like to determine the values of the two unknown parameters κ and a which appear in these equations.

The data can be analyzed most conveniently by eliminating the radius R between (5) and (6). Multiplication of (5) by (6) yields the relation

$$vE=B[\eta-(7/4)](\eta-\tfrac{1}{4}), \quad \text{where} \quad B\equiv\rho\kappa^3/8\pi. \tag{8}$$

Since $\eta\gg1$, (8) gives to good approximation $\eta=(vE/B)^{1/2}+1$. Furthermore, (7) and (5) give

$$\eta=\ln\{16E[\rho\kappa^2 a(\eta-7/4)]^{-1}\}. \tag{9}$$

A combination of these results yields then the relation

$$(vE)^{1/2}=B^{1/2}\left\{\ln E-\ln\left[\left(\frac{vE}{B}\right)^{1/2}-\frac{3}{4}\right]\right\}+B^{1/2}\left[\ln\left(\frac{16}{\rho\kappa^2 a}\right)-1\right]. \tag{10}$$

Since vE is, by (8), only a slowly varying function of E, the logarithmic second term in the curly brackets is in first approximation almost a constant. Hence a plot of $(vE)^{1/2}$ versus $\ln E$ should, in this approximation, yield a straight line of slope $B^{1/2}$. In next approximation, one can use the approximate value of B thus determined in the curly brackets; a plot of $(vE)^{1/2}$ versus the expression in curly brackets should thus yield a straight line of slope $B^{1/2}$ (which determines κ) and with an intercept which determines a. If the experimental data are plotted in this way, they do indeed appear to fall on a straight line whose slope and intercept yield the values

$$\kappa=(1.00\pm0.03)\times10^{-3}\ \text{cm}^2\ \text{sec}^{-1}, \tag{11}$$

$$a=(1.28\pm0.13)\ \text{Å}, \tag{12}$$

with estimated probable errors as indicated.[16] Here we have used $\rho=0.1454$ g cm^{-3} for the density of liquid helium.

It is striking that the value of κ deduced in (11) from

[13] This can be demonstrated visually quite vividly by experiments in which a buoyant vortex ring consisting of a light liquid is formed in a heavier liquid. See J. S. Turner, Proc. Roy. Soc. (London) **A239**, 61 (1957).

[14] H. Lamb, *Hydrodynamics* (Dover Publications, Inc., New York, 1945), 6th ed., p. 241. See also L. Prandtl and O. G. Tietjens, *Fundamentals of Hydro- and Aeromechanics* (Dover Publications, Inc., New York, 1957), Chap. 12. By virtue of the electromagnetic analogy mentioned in footnote 6, the energy E in (5) is analogous to the energy $\frac{1}{2}LI^2$ associated with the self-inductance L of a circular current loop.

[15] The relations (5) and (6) are derived assuming that the vorticity has a constant value inside the core. If one assumes instead that the core is hollow so that the vorticity vanishes there, then the formulas (5) and (6) differ by replacing η by $\eta-\frac{1}{4}$. [See W. M. Hicks, Phil. Trans. Roy. Soc. **175A**, 183 and 190 (1884).] Since the density of the fluid must decrease when the velocity v_s becomes sufficiently high, this second model might be slightly preferable. But since $R\gg a$ and $\eta\approx10$ in our experiments, the distinction between the two models is essentially negligible and is physically rather meaningless since the hydrodynamic approximation cannot be extended reliably down to the atomic scale of a.

[16] If one assumes a hollow core, only the intercept of the straight line (10) is affected (-1 being replaced by $-5/4$). Hence this model gives the same value of κ, but a somewhat smaller hollow core radius $a=(1.00\pm0.10)$ Å.

the experimental data is, within the limits of estimated error, equal to one quantum κ_0 of circulation given by (3).[17] To make the comparison between theory and experiment more explicit, one can assume that the charge carriers are vortex rings with a circulation κ equal to precisely one quantum κ_0 and can choose for the only remaining parameter a [on which (5) and (6) depend only insensitively] a value of the order of (12). The equations (5) and (6) yield then a unique prediction for v and E for various values of R. The resulting theoretical curve of v versus E is shown in Fig. 2 together with the experimentally measured values. The agreement between theory and experiment is seen to be quite good. In the investigated experimental range where E is between 1.5 and 45 eV, the corresponding radius R of a vortex ring lies between 5×10^{-6} and 10^{-4} cm. It is also worth noting that the experimental data for both positive and negative charge carriers fall on the same curve (despite the fact that the mobility measurements in the limit of very low electric fields have shown appreciable differences between the mobilities of positive and negative ions)[2]. This is in agreement with what one would expect for a vortex ring since E and v are then determined by the properties of a large amount of fluid, rather than by the particular small charge coupled to it. All these results indicate that the charge carriers observed in the present experiments are indeed quantized charged vortex rings moving in the superfluid.

The core radius a in (12) is, as expected,[5] of the order of atomic dimensions. From experiments on the velocity of vortex waves Hall has inferred that the core radius of a free vortex line is approximately 6.8 Å, a value of the same order of magnitude as that in (12).[18] On the other hand, Vinen[9] in his experiment on quantized circulation used equilibrium free energy arguments to infer for a an unreasonably large value greater than 10^4 Å; he was thus led to suggest that the simple picture of free vortex lines is inadequate. The present experiments, however, do not support this suggestion since the simple model of free vortex rings with $a\approx1$ Å seems to fit our experimentally measured energies and velocities very well.

B. Speculative Remarks

Before discussing further experiments involving quantized vortex rings, it may be useful to interject a few speculative comments about the coupling of the charge to a vortex ring and about the initial formation of the ring. Let us begin by considering the first question from a phenomenological point of view, keeping in mind the fact that the vortex rings actually observed are fairly macroscopic ($R\gtrsim500$ Å). It is then most likely that the singular region in the fluid, i.e., the core of the vortex ring, acts as a potential well for the charge. In this case the charge, whether it be an ion or electron, is characterized by a wave function localized around the core. This wave function may, of course, extend somewhat beyond the confines of the core proper to a distance $r>a$, and may do so by different amounts for a positive or negative charge coupled to the ring. (The binding energy of either kind of charge to the core may correspondingly also be different, as long as it is sufficiently large to keep the charge coupled to the ring. The experiments performed up to now give no information about such details.) As far as motion along the circumference of the core is concerned, the potential well acts like a one-dimensional box of length greater than 1000 Å. Corresponding to this degree of freedom, the spacing of the energy levels of the charge is thus much less than kT. The charge can, therefore, be regarded as moving around the circumference like a classical particle. Even if its effective mass is of the order of 100 He-atom masses,[19] its thermal velocity is large enough so that the fractional change in the velocity v of the vortex ring is always small during the time required for the charge to traverse the circumference. In addition, the motion of the charge on the ring is randomly interrupted by collisions with thermal excitations, its mean free path (estimated from the ion mobility measurements) being comparable to the circumference. Hence the charge can be regarded as being in effect distributed uniformly around the core of the vortex ring.

Let us next conjecture why the core should act as a potential well for the charge. The following model may illuminate the essential features of a mechanism. The electric field of an ion immersed in liquid helium compresses the liquid in its immediate vicinity appreciably; indeed, this electrostriction should be sufficient to cause the solidification of the liquid within a radial distance of the order of 7 Å from the ion.[19] Consider then a small solid sphere of this kind (which we shall call an "ion complex") in the vicinity of a vortex ring. The fluid velocity due to the vortex is greatest near the core and falls off with increasing distance from the core; correspondingly, it follows by Bernoulli's principle that the pressure in the fluid is least near the core and increases with distance from the core. The net pressure force acting on the small solid sphere surrounding the ion tends therefore to drive it toward the core. Indeed, if the sphere is located in the core, it replaces a corresponding volume of fluid rotating with high velocity and reduces thereby the kinetic energy associated with

[17] This value is based upon the plausible assumption that the charge carriers (arising from the He^+ ions and electrons originally produced near the source) are singly charged. If they were doubly charged, one would expect that some of them would also be singly charged; but experimentally the data for all charge carriers, including those of opposite sign, fall on the same curve. Furthermore, the deduced value of κ would then be $2^{1/3}\kappa_0$, which seems rather unlikely.

[18] H. E. Hall, *Advances in Physics* (Francis & Taylor, Ltd., London, 1960), Vol. 9, p. 89. It is possible that the presence of a charge (coupled to the vortex ring as described in the following paragraphs) may modify somewhat the effective core radius a compared to that of an uncharged vortex.

[19] K. R. Atkins, Phys. Rev. **116**, 1339 (1959).

the vortex ring[20]; hence, the situation of lower total energy is one where the little sphere is located at the core rather than elsewhere in the fluid.[21] (In the case of an electron in liquid helium, the theory has been advanced that it surrounds itself by a hollow bubble in order to reduce its zero point kinetic energy[22]; here again the vortex core, which tends to be hollow already, would form an energetically favorable region for trapping the electron.)

Finally we comment on the initial creation of the vortex ring by the original ion complex. Although the problem here is somewhat delicate because arguments of macroscopic hydrodynamics become questionable when applied to vortex rings of atomic size, the process is likely to be analogous to that involved in the creation of a vortex ring behind a sufficiently rapidly moving macroscopic sphere.[23] The smallest vortex ring thus created must have a radius of the order of a few angstroms (the size of the ion-complex sphere). Since the vortex ring has one quantum of circulation and is of a size not much larger than a roton excitation, the critical velocity v_c which the ion complex must attain to create the vortex ring with conservation of energy and momentum should be comparable to that necessary for creation of a roton, i.e., $v_c \approx 50$ m/sec. This velocity is of the order of magnitude of that attained by an ion-complex between collisions with excitations if the temperature T and electric field $\mathcal{E}$ are such that $e\mathcal{E}l \gtrsim kT$. (Indeed, drift velocities of the order of 40 m/sec were the highest ones observed by Reif and Meyer before their apparatus failed to function because of the appearance of frictionless behavior of the charge carriers.)[24] When the ion complex is initially accelerated, it attains first the energy necessary to create a vortex ring of one quantum of circulation, gets captured by it, and then slows down. It is thus unlikely that the ion complex in our experimental situation can attain the larger energy necessary to create a vortex ring with several quanta of circulation before it creates the ring of minimum circulation h/m.

3. GENERAL DYNAMICAL PROPERTIES OF CHARGED VORTEX RINGS

A. Dispersion Relation

This section will be devoted to an investigation of the three-dimensional motion of charged vortex rings under the influence of external forces of arbitrary direction. Such studies provide not only further evidence that the observed charge carriers are vortex rings, but show also how the general dynamical behavior of such rings can be understood in detail.

The previous experiments have dealt only with the motion of vortex rings in one dimension. To good approximation the situation can then be described in the following simple terms. A vortex ring has associated with it a certain energy E given by (5) and a "momentum"[25]

$$\mathbf{p} = \pi\rho\kappa R^2 \mathbf{n}, \tag{13}$$

pointing along its axis in the direction (specified by the unit vector $\mathbf{n}$) of the flow velocity $\mathbf{v}_s$ at the center of the ring. Equation (6) is then, to good approximation, consistent with the general result

$$\mathbf{v} = \partial E/\partial \mathbf{p}, \tag{14}$$

relating the group velocity of any excitation to the gradient of its energy with respect to its momentum. (In our one-dimensional experiments $\mathbf{p}$ and $\mathbf{v}$ are always oriented along the direction $\mathbf{n}$ of the applied electric fields.) Furthermore, since η is a very insensitive function of R(or E), it can be regarded as nearly constant if the energy E does not vary over too large a range. In that case (5) and (13) imply the approximate "dispersion relation"

$$E = A p^{1/2}, \tag{15}$$

where $p \equiv |\mathbf{p}|$ and where A is a constant. This is to be contrasted with the dispersion relation $E \propto p^2$ for an ordinary particle. Equation (15) implies that $v \equiv |\mathbf{v}|$ given by (14) *de*creases as p *in*creases; indeed, $v = \frac{1}{2} A p^{-1/2} = \frac{1}{2} A^2 E^{-1}$ so that $v \propto E^{-1}$.

These considerations suggest that it should be possible to describe the general three-dimensional motion of a vortex ring in terms of a dispersion relation $E = E(p)$ relating its energy E to the magnitude p of its momentum by the Eqs. (5) and (13) [i.e., approximately by (15)]. The dynamics of a vortex ring should then be completely described in terms of the equation of motion $\dot{\mathbf{p}} = \mathbf{F}$ (where $\dot{\mathbf{p}} = d\mathbf{p}/dt$ and $\mathbf{F}$ is the external applied force) and the relation (14) connecting $\mathbf{v}$ and $\mathbf{p}$.

To check the validity of this general point of view and to provide further evidence that the unusual behavior of our charge carriers can be described in a consistent fashion, we designed the simple transverse deflection experiment illustrated in Fig. 4. This arrangement is similar to a cathode-ray oscilloscope. Charge carriers are given an energy $E_0 = eV_0$ by passing through an initial potential difference V_0 applied between the source S and the first grid A. The three slits (1 mm $\times$6 mm) in A, A_1, and A_2 serve to produce a well-

[20] *Very* crudely, by an amount of the order of 10^{-3} eV.

[21] We are indebted to Professor R. P. Feynman for discussing with us his thoughts on the subject and thereby helping to confirm our own speculative conclusions about the location of the charge on the ring.

[22] C. G. Kuper, Phys. Rev. **122**, 1007 (1961).

[23] See, for example, the lovely flow photographs of vortex formation in L. Prandtl and O. G. Tietjens, *Applied Hydro- and Aeromechanics* (Dover Publications, Inc., New York, 1957), p. 279. It should, however, be remembered that these photographs, although suggestive, are made by using a real fluid which exhibits viscous effects in the boundary layer.

[24] See Ref. 2; also *Liquid Helium*, edited by G. Careri (Academic Press Inc., New York, 1963), International School of Physics, Enrico Fermi, course 21, pp. 422 and 424.

[25] More precisely this is the "impulse." The distinction can be found elaborated by C. C. Lin in *Liquid Helium*, edited by G. Careri (Academic Press Inc., New York, 1963), International School of Physics, Enrico Fermi, course 21, pp. 98–103.

collimated charge-carrier beam of rectangular cross section. The beam passes then between a pair of deflecting plates of length L_z separated by a distance L_x. A potential V_x applied between these plates produces a small transverse electric field $\mathcal{E}_x$; as a result the beam is deflected through a net angle θ. Most conveniently one can measure the change in V_x required to deflect the beam through the particular angle which makes it pass first through one, and then through the other, of two slits in a mask M in front of the collector C. The experiment consists then of observing the current I at the collector C as a function of V_x for a given initial potential V_0.

Since the deflection angle θ is small, the experiment can be analyzed by a simple impulse approximation. A charge carrier arrives at the deflecting plates with an energy $E=eV_0$; it has then a momentum p_0 and a corresponding velocity v_0 in the z direction. As a result of passing between the deflecting plates, it acquires a small net momentum Δp_x in the x direction. Its final momentum $\mathbf{p}$ (and corresponding velocity $\mathbf{v}$) makes then an angle $\theta=\Delta p_x/p_0$ with respect to the z axis. (This means that the plane of the ring is tilted by this angle.) Let us first neglect edge effects by assuming that the field $\mathcal{E}_x$ has a constant value between the deflecting plates and falls abruptly to zero outside this region. Since $\Delta p_x \ll p_0$, the charge carrier spends then to good approximation a time L_z/v_0 between the plates and acquires as a result a transverse momentum $\Delta p_x=(e\mathcal{E}_x)(L_z/v_0)$. Thus

$$\theta=\frac{\Delta p_x}{p_0}=\frac{e\mathcal{E}_x(L_z/v_0)}{p_0}=\frac{eV_x}{p_0v_0}\frac{L_z}{L_x}, \tag{16}$$

since $\mathcal{E}_x=V_x/L_x$. If edge effects are taken into account, the momentum gain Δp_x calculated above should be multiplied by some geometrical correction factor g. Furthermore, (14) permits one to write quite generally for any excitation

$$pv=p(\partial E/\partial p)=\gamma E \quad (\gamma\equiv\partial \ln E/\partial \ln p). \tag{17}$$

Hence, one obtains the general result

$$\theta=\frac{g}{\gamma}\frac{V_x}{V_0}\frac{L_z}{L_x}, \tag{18}$$

where we have put $E_0=eV_0$.

If the charge carrier is an ordinary particle, then $E\propto p^2$ so that the parameter γ defined in (17) assumes the value $\gamma=2$. On the other hand, if it is a vortex ring, the relation $E\propto p^{1/2}$ of (15) gives $\gamma=\frac{1}{2}$. To good approximation the result (18) applied to vortex rings gives then

$$\gamma=\tfrac{1}{2} \quad \text{and} \quad \theta_v=4\theta_0, \tag{19}$$

where θ_v is the observed deflection angle of the vortex ring and θ_0 is the deflection angle which would be observed for ordinary particles under identical conditions.

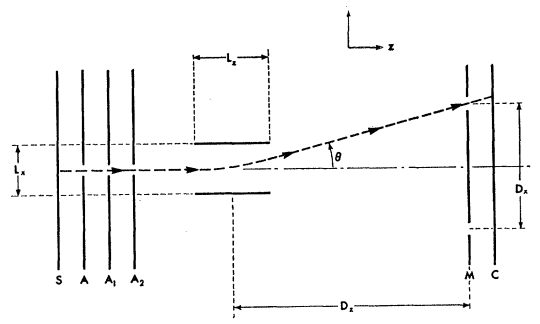

FIG. 4. Schematic diagram of the deflection apparatus. The deflection angle $\theta=\frac{1}{2}D_x/D_z=0.208$ rad. Other actual dimensions are $L_x=0.3$ cm, $L_z=0.5$ cm, and $D_z=1.25$ cm.

The correction factor g for edge effects can, actually, be calculated very readily. Consider the most general case of arbitrary spatial variation of the field $\mathcal{E}_x$ due to the deflection plates. Since it requires a time $dt=dz/v_0$ for the charge carrier to undergo a displacement with component dz in the z direction, the total transverse momentum acquired by the carrier is given by

$$\Delta p_x=\int e\mathcal{E}_x dt=\frac{e}{v_0}\int_{-\infty}^{\infty}\mathcal{E}_x dz. \tag{20}$$

But, by Gauss's theorem, the last integral must be equal to $4\pi Q'=4\pi C'V_x$ where Q' is the charge per unit length on one of the deflection plates (considered of infinite extension in the y direction) and where C' is the actual capacity per unit length of the pair of deflection plates. Thus one obtains

$$\theta=\frac{\Delta p_x}{p_0}=\frac{4\pi eC'V_x}{p_0v_0}=\frac{4\pi}{\gamma}\frac{V_x}{V_0}C'. \tag{21}$$

But $C'=gC_0'$, where $C_0'=L_z/(4\pi L_x)$ is the ideal capacitance per unit length in the absence of edge effects and where g is a correction factor whose calculation is a standard problem in electrostatics. [A Schwartz-Christoffel transformation gives in first approximation $g=1+b^{-1}(1+\ln b)$ where $b\equiv\pi L_z/L_x$.][26]

The actual experiment was carried out in the apparatus of dimensions indicated in Fig. 4. For any initial potential V_0 one could measure the potential V_x required to produce the fixed deflection angle θ. The experiment was carried out with both positive and negative charge carriers of several energies corresponding to initial voltages of magnitude $|V_0|$ between 5 and 45 V. As expected from (18), the ratio V_x/V_0 was found to be essentially constant ($V_x/V_0=0.046\pm0.002$). The value of the geometrical correction factor g calculated for the deflection plates alone was 1.59. To get an

[26] P. M. Morse and H. Feshbach, *Methods of Theoretical Physics* (McGraw-Hill Book Company, Inc., New York, 1953), Vol. 2, p. 1246. A more accurate result is quoted in A. H. Scott and H. L. Curtis, J. Res. Natl. Bur. Std. 22, 754 (1939).

improved value taking into account the presence of other electrodes like A_2, the electrode structure was drawn to scale with silver paint on resistance paper; this modified "electrolytic tank" analog technique permitted measurement of the electric field at all points and consequent numerical evaluation of the integral in (20). The best estimate thus obtained for g was $g=1.39\pm5\%$. Agreement with the theoretical expression (18) requires then that $\gamma=0.51\pm0.04$. This result is completely incompatible with the value $\gamma=2$ for an ordinary particle, but is in good agreement with the value $\gamma=\frac{1}{2}$ deduced in (19) for vortex rings.[27] The deflection experiment provides, therefore, additional evidence that the general dynamical behavior of the charge carriers can be consistently described in terms of the dispersion relation characteristic of vortex rings.

B. Magnus Forces

It is instructive to show how the dynamical behavior of charged vortex rings can be understood from a more detailed hydrodynamical point of view which provides appreciably greater physical insight. Our analysis will involve the hydrodynamic lift (or "Magnus") force.[28] Although the application of this result to the nonsteady motion of curved vortex filaments has not been rigorously established in classical hydrodynamics, it describes the observations quite well and justifies explicitly our previous description in terms of a dispersion relation.

The core of a charged vortex ring may be regarded as a charged thin solid ring of negligible mass; by Newton's second law of motion the net force on this body must then always vanish. But this force consists of two parts: (1) the applied force $\mathbf{F}$ due to external fields and (2) the hydrodynamic Magnus force. Thus the core must always move so that $\mathbf{F}+\mathbf{G}=0$ or

$$\mathbf{G}=-\mathbf{F}, \tag{22}$$

where the Magnus force $\mathbf{G}'$ per unit length will quite generally be assumed to be given by [28]

$$\mathbf{G}'=\rho\boldsymbol{\kappa}\times\mathbf{U}. \tag{23}$$

Here ρ is the density of the fluid, $\boldsymbol{\kappa}$ is the circulation vector of the element of core length under consideration (the direction of $\boldsymbol{\kappa}$ being such that the fluid in the vicinity of the element flows in a counterclockwise sense about this direction), and $\mathbf{U}$ is the relative velocity of this element with respect to the fluid. Thus $\mathbf{U}=\mathbf{u}-\mathbf{u}_f$, if $\mathbf{u}$ is the velocity of the core element and if $\mathbf{u}_f$ denotes the fluid velocity at this position caused by all sources other than this core element itself. Note that the relations (22) and (23) imply that a straight charged vortex line in the presence of an external force must always move so that $\mathbf{U}$ is perpendicular to this force.

In applying the relations (22) and (23) to a vortex ring, we shall assume that its core is constrained to remain always circular in shape.[29] As a result of external forces changes can, however, be produced not only in the velocity $\mathbf{v}$ of the center of this ring, but also in its radius R and in its axial direction $\mathbf{n}$ which specifies the orientation of the plane of the ring. By direct calculation it can be shown that the fluid velocity u_f at any core element due to the rest of the circular vortex ring is equal to $v\mathbf{n}$ where v is essentially given by (6). In considering the effect of an applied force $\mathbf{F}=e\mathcal{E}$ at any instant of time, one can resolve it into a component parallel to the axial direction $\mathbf{n}$ (which we shall choose as the $\hat{z}$ direction) and into a component (chosen to be in the $\hat{x}$ direction) parallel to the plane of the ring. We shall consider the effects of these components in turn.

When the applied force $\mathbf{F}$ is in the axial (or $\hat{z}$) direction, the Magnus force must, by (22), point in the opposite direction. Hence the relative velocity $\mathbf{U}$ must point along the outward radial direction of the ring see Fig. 5. The core velocity becomes then $\mathbf{u}=\mathbf{v}+\mathbf{U}$ where $\mathbf{v}=v\hat{z}$ is axial and the radial component $\mathbf{U}=\dot{R}\hat{R}$ tends to increase the radius of the ring in the course of time. The total Magnus force on the core is by (27) equal to $G_z=-\rho\kappa\dot{R}(2\pi R)$. Hence, (22) requires that the radial velocity $\dot{R}$ be

$$2\pi\rho\kappa R\dot{R}=(d/dt)(\pi\rho\kappa R^2)=F_z. \tag{24}$$

Since v is by (6) a decreasing function of R, the axial velocity $u_z=v$ of the ring *de*creases in time according to $du_z/dt=(dv/dR)\dot{R}$. Using (13) as a definition of the momentum $\mathbf{p}$, the relation (24) is equivalent to $\dot{p}_z=F_z$. Furthermore, the energy gain of the ring in time dt is equal to the work done on it by the applied force, i.e.,

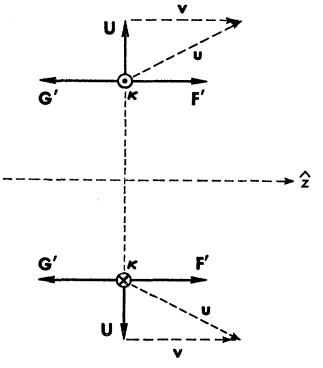

FIG. 5. Cross-sectional view of a vortex ring in the presence of an applied axial force $\mathbf{F}'$ per unit length. (The symbols ⊙ and ⊗ indicate that the circulation vector $\boldsymbol{\kappa}$ points out of, or into the paper, respectively.)

[27] A more accurate evaluation of $p(\partial E/\partial p)$ in (17) yields, by (5) and (13), $\gamma=\frac{1}{2}\{1+[\eta-(7/4)]^{-1}\}\approx0.56$ since $\eta\approx10$. The deflection experiment is not accurate enough to discriminate between this result and the simpler value $\gamma=\frac{1}{2}$.

[28] For a derivation of this hydrodynamic result see, for example, K. Oswatitsch, *Handbuch der Physik*, edited by S. Flügge (Springer-Verlag, Berlin, 1959), Vol. 8/1, p. 84. See also L. M. Milne-Thomson, *Theoretical Hydrodynamics* (Macmillan, Ltd., London, 1938), pp. 237–243, in particular the theorem of Blasius.

[29] We shall thus neglect vibrations of the ring or any effects due to a possible nonuniform distribution of charge along the core of the ring when it is in the presence of an electric field parallel to its plane.

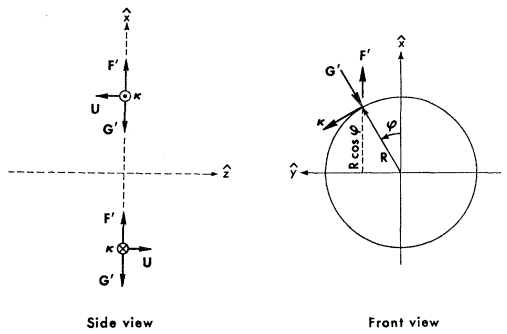

FIG. 6. Cross-sectional and frontal views of a vortex ring in the presence of a force $\mathbf{F}'$ per unit length applied in the $\hat{x}$ direction parallel to the plane of the ring. (The symbols $\odot$ and $\otimes$ indicate vectors pointing out of, or into, the paper, respectively.)

$dE=F_z u_z dt=\dot{p}_z(v_z dt)=dp_z v_z$ which is consistent with the relation (14).

When the applied force is in the $\hat{x}$ direction parallel to the plane of the ring, the Magnus force on each element of the core must have a component in the $-\hat{x}$ direction. The cross-section diagram of Fig. 6 shows then immediately that the relative velocities $\mathbf{U}$ of core elements on opposite sides of the ring must be equal but of opposite sign. As a result, the plane of the ring must thus rotate about the $\hat{y}$ axis. More precisely, the relative velocity $\mathbf{U}$ can have no radial component since this would lead to a Magnus force in the $\hat{z}$ direction in which there is no applied force. Hence the radius of the ring, and hence its energy, remains constant. Rotation of the plane of the ring about the $\hat{y}$ axis with angular velocity $\dot{\theta}$ produces, however, a relative core velocity $\mathbf{U}=-(R\cos\varphi)\dot{\theta}\hat{z}$ at a ring element of length $(Rd\varphi)$ making an angle φ with the $\hat{x}$ axis. The Magnus force on this element is then $-\rho\kappa R\cos\varphi\dot{\theta}(Rd\varphi)$ in the $\hat{R}$ direction. If this is multiplied by $\cos\varphi$ and integrated over all angles $0<\varphi<2\pi$, one obtains the total $\hat{x}$ component of the Magnus force on the ring. By virtue of (22), one obtains then the following relation for $\dot{\theta}$:

$$G_x=-\pi\rho\kappa R^2\dot{\theta}=-F_x. \tag{25}$$

Using the definition (13) of the momentum $\mathbf{p}$, (25) is equivalent to $|\mathbf{p}|\dot{\theta}=F_x$ or to $\dot{p}_x=F_x$ since $\dot{p}_x=|\mathbf{p}|\dot{\theta}$ when R is unchanged and the vector $\mathbf{p}$ simply rotates. Thus the situation is again consistent with our previous description in terms of a dispersion relation.

4. INTERACTION OF VORTEX RINGS WITH QUASIPARTICLES

A. Energy Loss Measurements

We already pointed out that at sufficiently low temperatures (say 0.28°K) a vortex ring subject to no external forces can traverse an appreciable distance with negligible loss of energy. At higher temperatures the energy loss does, however, become increasingly pronounced; e.g., at 0.65°K, it may amount to as much as 15 eV/cm. This energy loss can be attributed to the interaction of the vortex ring with the various quasiparticles in the liquid. These quasiparticles are expected to be phonons or residual He^3 impurities at low temperatures, but at higher temperatures they are predominantly rotons since the number of these increases exponentially. A systematic investigation of the energy losses of vortex rings at several temperatures should, therefore, allow one to study these scattering processes in detail and to deduce explicit values for the cross sections describing the scattering of these various quasiparticles by vortex lines.

The quantity of experimental interest is the effective frictional force $\mathcal{F}$ acting on a vortex ring because of the scattering of such quasiparticles. In the present context we shall again deal with the simple case where the vortex ring is moving in one dimension, say in the $\hat{z}$ direction. The force $\mathcal{F}$ acts then in the $-\hat{z}$ direction and is related to the vortex ring energy loss per unit distance traveled by the ring, i.e., $\mathcal{F}=(-dE/dz)$. This frictional force is, of course, some function of the temperature T and of the energy E of the ring. It is, however, readily possible to infer the functional form of $\mathcal{F}$ on the basis of a very general argument. Suppose that a long straight vortex line moves with velocity v relative to the quasiparticles of the fluid (the velocity v being very small compared to the mean speed of the quasiparticles). The frictional force $\mathcal{F}'$ per unit length of the line must vanish when $v=0$. If $\mathcal{F}'$ is expanded in a power series in v, the leading term of appreciable magnitude is then proportional to v; i.e., $\mathcal{F}'\propto v$. [Since the mean free paths of all quasiparticles are known to be large, greater than 10^{-4} cm at the temperatures below 0.7°K of our experiments,[30] the force can be calculated by using kinetic theory to analyze individual scattering processes of quasiparticles with a vortex line (see Appendix II).] But the radius R of a vortex ring is large ($R>500$ Å in the present experiments) compared to the distance over which a vortex line interacts appreciably with a quasiparticle and also large compared to the wavelength λ of a quasiparticle.[31] Hence the frictional force on a vortex ring must be the same as that on a vortex line bent into a circle of radius R, i.e., $\mathcal{F}=(2\pi R)\mathcal{F}'\propto Rv$. The expression (6) for v shows then that $\mathcal{F}$ is almost independent of the radius R, or energy E, of the ring. More precisely, $\mathcal{F}$ can be written in the form

$$\mathcal{F}=-dE/dz=\alpha(T)\chi(E)\quad(\chi\equiv\eta-\tfrac{1}{4}). \tag{26}$$

Here χ depends on E only logarithmically by virtue of (9), while α is some coefficient which, for a ring of given circulation, can only depend on T. The relation (26) separates explicitly the dependence of $\mathcal{F}$ on energy and temperature. Since (5) and (7) permit calculation

[30] K. R. Atkins, *Liquid Helium* (Cambridge University Press, New York, 1959), p. 109.

[31] This is certainly true for rotons ($\lambda\approx 1$ Å) and He^3 atoms; it is also approximately true for most vortex rings in the case of phonons where $\lambda\lesssim 400$ Å at 0.3°K.

of E and η for various values of R, the dependence of $\chi(E)$ on E can be calculated explicitly (e.g., when $R=5000$ Å, $E=19.5$ eV and $\chi=10.1$).

Two methods were used to measure the frictional force $\mathfrak{F}$. The first of these (which we shall call the "constant-velocity method") is based upon the compensation of the frictional losses by a known applied electric field. The basic apparatus is the two-stage velocity spectrometer of Fig. 1(b) where the velocity can be measured either in the region Γ_1 or the region Γ_2. In the absence of any applied dc electric fields, a vortex ring loses energy in traversing the spectrometer so that its measured velocity is greater in the region Γ_2 than in the region Γ_1. It is, however, possible to apply a constant uniform electric field $\mathcal{E}$ throughout both Γ_1 and Γ_2, and to adjust $\mathcal{E}$ until the measured velocity is the same in both Γ_1 and Γ_2. Under these circumstances the vortex ring does not lose any energy in traversing the apparatus and the applied force just balances the frictional force so that $\mathfrak{F}=e\mathcal{E}$. The energy of the ring can be computed from its measured velocity if it is assumed that the relation between v and E determined in Sec. 2 of this paper is a characteristic temperature-independent property of vortex rings. (This energy E is somewhat less than that given by the initial potential between C and grid A_1, but the difference is consistent with the energy loss caused by the measured friction force $\mathfrak{F}$.)

Figure 7 shows experimental values of $\mathfrak{F}$ measured by this method at a given temperature $T=0.615$°K for vortex rings of various energies. It is seen that the data are indeed consistent with the very insensitive energy dependence expected from (26). A plot of $\mathfrak{F}$ versus $\chi(E)$ gives the value of $\alpha(T)$ at the given temperature of the experiment (e.g., $\alpha=1.04$ eV/cm at $T=0.615$°K). The solid circles in Fig. 9 show values of α obtained at several temperatures by this method. Small values of α cannot be measured accurately because of the difficulty of resolving small changes in velocity between the regions Γ_1 and Γ_2. (The small energy loss becomes then comparable to the energy gained from the alternating electric square-wave field.)

The second method of measuring $\mathfrak{F}$ (the "stopping-potential method") attempts to determine the energy loss suffered by a vortex ring in traversing a long field-free region and is more accurate at low temperatures where α is small. In Fig. 8 the field-free region of length L is contained between the grids A_1 and A_2. The initial energy E_1 of the ring entering this region at A_1 is measured by the magnitude V_1 of the potential applied between the source S and A_1; the final energy E_2 of the ring leaving the region at A_2 is measured by the magnitude V_2 of the opposing potential which, when applied between A_2 and C, is just sufficient to prevent charge carriers from reaching the collector C. The spacing L_1 between SA_1 and between A_2C is appreciably smaller than L. By virtue of (26), the energy E_1 is given by $E_1=eV_1-\alpha\langle\chi\rangle_1 L_1$, where $\langle\chi\rangle_1$ is a suitable average of $\chi(E)$ over the energy range extending from $E=0$ to $E=E_1$. In Appendix I it is shown that to good approximation $\langle\chi\rangle_1=\chi_1-1$ where χ_1 is the value of $\chi(E)$ for $E=eV_1$. Similarly the energy E_2 is given by $E_2=eV_2+\alpha\langle\chi\rangle_2 L_1$. Here $\langle\chi\rangle_2$ is the same kind of average of $\chi(E)$ over the energy range between 0 and E_2, so that $\langle\chi\rangle_2=\chi_2-1$, where χ_2 is the value of $\chi(E)$ for $E=eV_2$. The energy loss in the drift region between A_1 and A_2 can, by (26), be written as $E_1-E_2=\alpha\bar{\chi}L$ where we have used the fact that $\chi(E)$ is a very slowly varying function of E to replace it by its mean value in this region; one can put $\bar{\chi}=\frac{1}{2}(\chi_1+\chi_2)$ to excellent approximation.[32] Eliminating E_1 and E_2 between these relations one can thus calculate α at the particular temperature of the experiment from the expression

$$\alpha=\frac{e(V_1-V_2)}{\frac{1}{2}(\chi_1+\chi_2)(L+2L_1)-2L_1}. \tag{27}$$

The stopping potential V_2 was determined by observing the current I to the collector C as a function of the voltage V between A_2 and C. The experimentally observed current I does not fall abruptly to zero at a sharply defined value $V=V_2$, but exhibits a more gradual cutoff characteristic. It was, therefore, necessary to use a systematic extrapolation method to estimate the potential V_2 corresponding to essentially complete suppression of the collector current I.[11] This procedure proved to be reproducible and consistent. Its consistency could be checked by the following facts: (1) The energy dependence of $\mathfrak{F}$ determined in this way by the present method varied properly as $\chi(E)$, as expected from (26) and from the experimental measurements of the constant-velocity method. (2) The values of $\alpha(T)$ measured by the present method were in good agreement with those obtained by the constant-velocity method as can be seen in Fig. 9.

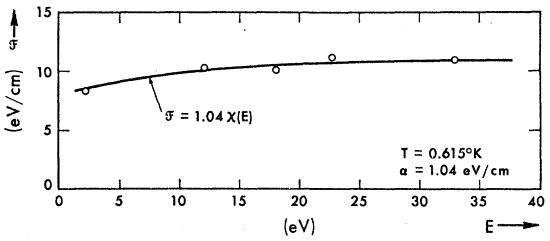

FIG. 7. The frictional force $\mathfrak{F}$ on a vortex ring as a function of its energy E at a given temperature $T=0.615$°K.

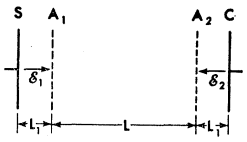

FIG. 8. Schematic diagram illustrating the stopping-potential method of measuring the energy loss of vortex rings ($L_1=0.3$ cm, $L=2$ cm).

[32] The fractional error involved in this approximation is at most of the order of $(V_1-V_2)^2/(4\bar{\chi}V_1V_2)$ which is small since $\bar{\chi}$ is of the order of 10.

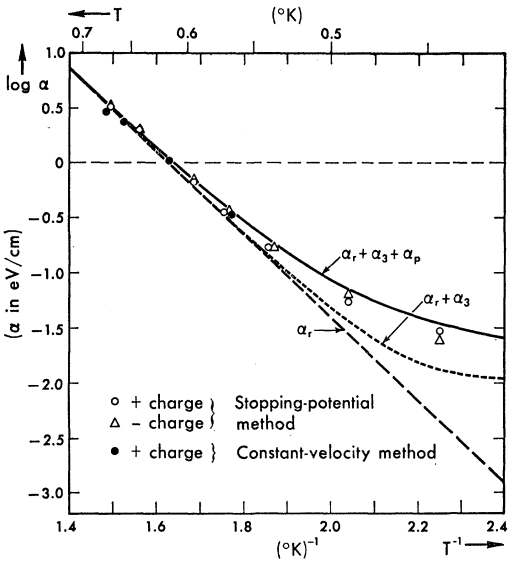

FIG. 9. Logarithmic plot showing for both positively and negatively charged vortex rings the dependence of the attenuation coefficient α as a function of T^{-1}. The dashed curve shows the behavior of α expected from roton scattering alone; the dotted curve that expected from both roton and He^3 impurity scattering; the solid curve that expected if phonon scattering of the predicted magnitude is also included.

At high temperatures where α is large, the considerable energy loss in the main drift space A_1A_2 was partially compensated by applying a potential V across this space. [An extra term eV should then be added to the numerator of (27).] At the other extreme of low temperatures, where α is so small that the energy loss in the main drift space is of the order of 0.3 eV or less, the method tends to become inaccurate. The main reason is that an apparent accumulation of electric surface charge on the source electrode can introduce uncertainties of this order of magnitude in the measurement of the vortex ring energies. In determining V_2, a systematic attempt was made to correct for such "charging effects."[11] The values of α thus determined for both positive and negative vortex rings are shown in Fig. 9 and are in good agreement with each other.

B. Roton Scattering

The number of thermally excited rotons increases exponentially with increasing temperature, i.e., proportionately to $\exp(-\Delta/kT)$, where Δ is essentially the energy necessary to create a roton ($\Delta/k=8.65°K$).[33] The energy loss of vortex rings by roton scattering should, therefore, be predominant at relatively high temperatures. The corresponding attenuation factor α should accordingly be proportional to the mean number of rotons present and to some effective momentum-transfer cross section $\bar{\sigma}_{r0}$ describing the scattering of a roton by a vortex line. (Note that, in describing the scattering by a vortex *line*, the cross section $\bar{\sigma}$ has the dimensions of a length and represents some effective width of the line responsible for scattering.) The detailed calculation of Appendix II yields the result

$$\alpha_r=\frac{3\pi^2}{8}\frac{\kappa}{h^3}p_0^4e^{-\Delta/kT}\bar{\sigma}_{r0}(T), \tag{28}$$

where $\bar{\sigma}_{r0}$ is precisely defined by (A18), p_0 is the momentum of a roton with energy $\Delta(p_0/\hbar=1.92\times10^8\ cm^{-1})$,[33] and κ is the circulation of the vortex ring ($\kappa=h/m$ in our case of one quantum). The exponential factor in (28) predominates over any possible slow temperature dependence of $\bar{\sigma}_{r0}$. In the following we shall assume $\bar{\sigma}_{r0}$ to be temperature-independent. The experimental points of $\log\alpha$ versus T^{-1} in Fig. 9 indicate that at high temperatures α does indeed reflect the exponential temperature dependence expected by (28). At the highest temperature of the plot (0.67°K) the scattering should be due almost entirely to rotons. One can thus use the experimental data at this temperature to deduce from (28) the magnitude of the cross section for scattering by rotons. Thus one finds

$$\bar{\sigma}_{r0}=9.5\pm0.7\ \text{Å}. \tag{29}$$

At lower temperatures the experimental points of $\ln\alpha$ versus T^{-1} in Fig. 9 deviate increasingly from the straight line, presumably because interaction with other quasiparticles (phonons and He^3 impurities) becomes predominant. Before discussing these other scattering mechanisms, it is worth commenting on the value of $\bar{\sigma}_{r0}$ deduced in (29) from the present experiments. A cross section for the scattering of rotons by vortex lines can also be inferred from experiments on the attenuation of second sound[34] and on vortex waves in rotating liquid-helium II.[35] Hall gives a review of this work[35] which leads to an estimated cross section of about 10 Å. This value is in good agreement with the one obtained in (29) from the present experiments.

Several attempts have been made to deduce a value for $\bar{\sigma}_{r0}$ on the basis of microscopic arguments. Hall and Vinen[34,35] assumed that the predominant interaction between a roton and a vortex line is given by the expression $\mathbf{p}\cdot\mathbf{v}_s$ by which the energy of a roton of momentum $\mathbf{p}$ is increased when it finds itself in a superfluid which is not at rest, but is moving with a velocity $\mathbf{v}_s$; here $\mathbf{v}_s$ is the velocity (4) due to the vortex line. They used a Born approximation, which is of questionable validity and which suffers from some convergence difficulties, but they obtained order of magnitude agreement with the experimentally deduced value of $\bar{\sigma}_{r0}$; they also predicted it to be proportional to T^{-1}.

[33] J. L. Yarnell, G. P. Arnold, P. J. Bendt, and E. C. Kerr, Phys. Rev. **113**, 1379 (1959).

[34] H. E. Hall and W. F. Vinen, Proc. Roy. Soc. (London) **A238**, 204 (1956).

[35] H. E. Hall, *Advances in Physics* (Francis & Taylor, Ltd., London, 1960), Vol. 9, p. 89; see particularly pp. 111 and 126.

Lifshitz and Pitaevskii,[36] on the other hand, used a "quasiclassical" approximation to calculate $\bar{\sigma}_{r0}$. They found a temperature-independent cross section an order of magnitude too small and predicted also an appreciable amount of nonisotropic scattering. To account for the discrepancy they suggested, in addition to the $\mathbf{p}\cdot\mathbf{v}_s$ interaction, the existence of a predominant hard-core strong interaction effective only if a roton passes very close to the vortex line and leading to a temperature-independent cross section. None of these calculations can be considered really satisfactory and there is nothing in the present experiments which would tend to favor one of these calculations over the other.

C. He^3 Scattering

The interaction of vortex rings with He^3 atoms is of interest both intrinsically and because such scattering, due to the small number of He^3 impurity atoms present in ordinary liquid helium, becomes the predominant mechanism responsible for the friction force $\mathcal{F}$ at sufficiently low temperatures. The general expressions for the force $\mathcal{F}$ due to He^3 scattering is again expected to be of the form (26) with a corresponding attenuation factor α_3 derived in (A20) of Appendix II and given by

$$\alpha_3=\tfrac{3}{8}\kappa(2\pi m^* kT)^{1/2}n_3\bar{\sigma}_{30}(T). \qquad (30)$$

Here n_3 is the number of He^3 atoms per unit volume, m^* is the effective mass of such an atom (where m^* may be different from the actual mass m_3 of a He^3 atom), and $\bar{\sigma}_{30}$ is an effective cross section describing the scattering of a He^3 atom by a vortex line.

In order to measure α_3 experimentally, a known small quantity of He^3 was added to the He^4 gas which was later condensed to form the liquid under investigation. The fractional He^3 impurity concentration used was 28.4×10^{-6}. This concentration was subsequently also checked by mass-spectrometric analysis and was found to agree within 3%. The measurements of the friction force were carried out by the stopping-potential method at 0.28°K. At this low temperature the energy loss caused by rotons or phonons is quite negligible compared to that caused by the relatively numerous He^3 impurities so that the measured friction force $\mathcal{F}$ is due entirely to these impurities. These measurements verified again the weak energy dependence of $\mathcal{F}$ given by $\chi(E)$ in (26) and yielded the result $\alpha_3=(1.46\pm0.01)$ eV/cm. The relation (30) leads then at 0.28°K to an effective cross section

$$\bar{\sigma}_{30}=18.3\pm0.7\ \text{Å}, \qquad (31)$$

if one assumes for the effective mass the value $m^*=2.5m_3$ deduced from experiments on the propagation of second sound in He^4–He^3 mixtures.[37]

A further experiment was carried out to verify that the observed scattering was indeed due to He^3 atoms and that α_3 was properly proportional to the He^3 concentration n_3 as expected by (30). The previous sample was therefore diluted with ordinary helium (well helium with an estimated natural isotropic He^3 concentration of 1.4×10^{-7}) to give a new sample with a He^3 concentration of 7.55×10^{-6}, i.e., smaller than the concentration of the previous sample by a factor of 0.27. The value of α_3 measured in this sample at 0.28°K was $\alpha_3=(0.42\pm0.02)$ eV/cm, smaller than the value of α_3 in the previous sample by a factor of 0.28. This verifies the proportionality $\alpha_3\propto n_3$ within the limits of estimated error and supports the consistent interpretation of these experiments in terms of He^3 scattering with a cross section given by (31).

This diluted sample was also used to verify the additivity of He^3 and roton scattering by performing an experiment at the relatively high temperature of 0.61°K. The directly measured value of α was then $\alpha=1.42$ eV/cm. Roton scattering alone at this temperature should, by Fig. 9, contribute a value $\alpha_r=0.87$ eV/cm while (30) predicts for scattering by He^3 atoms (assuming $\bar{\sigma}_{30}$ to be temperature-independent) a value $\alpha_3=0.62$ eV/cm. The sum $\alpha_r+\alpha_3=1.49$ is thus in reasonably good agreement with the directly measured value of α.

The value of $\bar{\sigma}_{30}$ in (31) cannot be compared with data obtained from other experiments since we know of none which have attempted to measure the scattering between vortex lines and He^3 atoms. Such experiments on second sound propagation or vortex waves in rotating liquid helium containing He^3 impurities would, of course, be possible.

D. Comments on Photon Scattering

The approximate isotopic abundance of He^3 atoms in ordinary helium (obtained from wells) corresponds to a He^3 atom concentration[38] of 1.4×10^{-7} and is sufficient to lead at 0.28°K to a calculated value $\alpha_3=7.2\times10^{-3}$ eV/cm in our "pure" helium. This value of α is far greater than that due to rotons at this low temperature and is consistent with the estimated magnitude of the rate of energy loss observed for vortex rings at 0.28°K. The relation (30) shows that $\alpha_3\propto T^{1/2}$ if $\bar{\sigma}_{30}$ is assumed to be temperature-independent. The dotted curve in Fig. 9 illustrates then the predicted temperature dependence of the total attenuation coefficient $(\alpha_r+\alpha_3)$ if both roton and He^3 impurity scattering are taken into account.

[36] E. M. Lifshitz and L. P. Pitaevskii, Zh. Eksperim. i Teor. Fiz. **33**, 535 (1959) [English transl.: Soviet Phys.—JETP **6**, 418 (1957)].

[37] H. C. Kramers, in *Liquid Helium*, edited by G. Careri (Academic Press Inc., New York, 1963), International School of Physics, Enrico Fermi, course 21, p. 395. See also K. R. Atkins, *Liquid Helium* (Cambridge University Press, New York, 1959), p. 289.

[38] K. R. Atkins, Ref. 30, p. 230.

Finally, we turn to a discussion of the expected interaction of vortex rings with phonons. The analysis of Appendix II yields for the attenuation coefficient due to phonons the result

$$\alpha_p=\frac{\pi^2}{20}\frac{\kappa}{h^3}\left(\frac{kT}{c}\right)^4\bar{\sigma}_{p0}. \tag{32}$$

Pitaievskii[39] has attempted to calculate the momentum-transfer cross section of a phonon of momentum p by a vortex line and finds $\sigma_{p0}=(\pi/2)(\kappa^2p/c^2h)$. Equation (A18) of Appendix II gives then at 0.28°K an effective phonon cross section $\bar{\sigma}_{p0}=0.3$ Å; correspondingly $\alpha_p=2.2\times10^{-3}$ eV/cm, a value about 30% of the attenuation coefficient α_3 due to He^3 impurities. Because of its rapid temperature dependence α_p should, however, become more important than α_3 at higher temperatures and should be noticeable until, at temperatures appreciably above 0.5°K, it becomes insignificant compared to the coefficient α_r due to roton scattering. It was pointed out previously that measurements of the attenuation coefficient α become increasingly inaccurate at low temperatures where α is small. Nevertheless, the experimental points in Fig. 9 are seen to be not inconsistent with the theoretical solid curve obtained by adding to the attenuation coefficient $(\alpha_r+\alpha_3)$ due to rotons and He^3 impurities the phonon contribution α_p calculated by (31) on the basis of Pitaevskii's theory of the phonon-scattering cross section.

5. CONCLUDING REMARKS

The previous pages have presented evidence showing that it is possible to create charged vortex rings in liquid helium. Since these are created in the middle of the liquid, far from the disturbing effects of any walls, and since their charge allows them to be manipulated by external electromagnetic fields, the properties of these vortex rings can then be studied in considerable detail. In particular, we have discussed experiments showing that their circulation is equal to one quantum h/m; we have investigated their dynamical properties and found them to be consistent with those expected from hydrodynamical considerations; and we have studied their scattering by rotons and He^3 impurities and thus determined the scattering cross sections describing the interaction of these quasiparticles with vortex lines.

We are interested in pursuing a number of other experiments. For example, it would be desirable to determine the magnitude of the binding energy coupling the charge to the vortex ring. (A measurement of this kind might also have a bearing on other experiments suggesting a trapping of ions by vortex lines.[40]) It would also be interesting to devise an experimental arrangement which would favor the creation of vortex rings with more than one quantum of circulation.

ACKNOWLEDGMENTS

We wish to acknowledge several discussions with Professor J. J. Hopfield and Dr. A. L. Fetter, and to thank Dr. M. H. Lambert for calibrating our germanium resistance thermometer.

APPENDIX I: ENERGY GAIN IN THE STOPPING-POTENTIAL METHOD

We do not see what connection, if any, there might exist between our present experiments and the discrete discontinuities in ionic mobilities observed by Careri *et al.*[41] in superfluid helium at much higher temperatures. The latter authors suggested at one time that their results might be interpreted in terms of the creation of quantized vortex rings, although they pointed out that the estimated orders of magnitude involved in this explanation were rather inconsistent.[41] Later they suggested a more complicated hydrodynamical explanation.[42] It should also be pointed out that discrete discontinuities in ionic mobilities have recently been observed in ordinary liquids like argon and nitrogen.[43]

On the other hand, it seems likely that the very small deflection of ions observed by Careri *et al.*[44] in a magnetic field in superfluid helium at 0.2°K was due to the fact that these workers were not observing ordinary ions, but the charged vortex rings created by them. The velocities of vortex rings tend to be so small that the Lorentz force exerted on them by a magnetic field is ordinarily quite negligible. Recent experiments by Meyer[45] at 0.4°K have verified explicitly that the magnetic deflection of charge carriers is negligible when the latter have been given enough energy to exhibit vortex ring behavior.

Consider the space between S and A_1 in Fig. 8. An applied potential V_1 between these electrodes produces a field $\mathcal{E}_1=V_1/L_1$. The energy E of a vortex ring starting out near S is essentially zero. Taking into account the frictional force (26), one can then write

$$dE/dz=e\mathcal{E}_1-\alpha\chi(E) \tag{A1}$$

[39] L. Pitaevskii, Zh. Eksperim. i Toer. Fiz. **35**, 1271 (1957) [English transl.: Soviet Phys.—JETP **8**, 888 (1959)], particularly Eq. (29). See also A. L. Fetter (to be published).

[40] G. Careri, W. D. McCormick, and F. Scaramuzzi, Phys. Letters **1**, 61, (1962); also *Proceedings of the 8th International Conference on Low Temperature Physics* (Butterworths Scientific Publications, Ltd., London, 1963), p. 88.

[41] G. Careri, S. Cunsolo, and P. Mazzoldi, Phys. Rev. Letters **7**, 151 (1961).

[42] G. Careri, S. Cunsolo, and P. Mazzoldi, *Proceedings of the 8th International Conference on Low Temperature Physics* (Butterworths Scientific Publications, Ltd., London, 1963), p. 90.

[43] B. L. Henson, Phys. Rev. **135**, A1002 (1964).

[44] G. Careri, F. Dupré, and I. Modena, Nuovo Cimento **22**, 318 (1961).

[45] L. Meyer (private communication). We wish to thank Professor Meyer for permission to mention his unpublished results.

or

$$e\mathcal{E}_1 dz = dE\left(1-\frac{\alpha\chi}{e\mathcal{E}_1}\right)^{-1} \approx dE\left(1+\frac{\alpha\chi}{e\mathcal{E}_1}\right),$$

where we have assumed that the frictional force is relatively small so that $\alpha\chi \ll e\mathcal{E}_1$. After integration this becomes, putting $\mathcal{E}_1 L_1 = V_1$,

$$eV_1 = E_1 + \frac{\alpha L_1}{eV_1}\int_0^{E_1} \chi(E)dE. \tag{A2}$$

But (9) shows that $\chi \equiv \eta - \frac{1}{4}$ has to good approximation the functional form $\chi = c + \ln E$, where c is some constant. Integration of this expression gives the result[46]

$$\int_0^{E_1} \chi(E)dE = [\chi(E_1)-1]E_1 \approx (\chi_1 - 1)E_1, \tag{A3}$$

where we have used the approximation of putting $\chi(E_1) = \chi(eV_1) \equiv \chi_1$ in the last step since χ is a slowly varying function of E. Substituting (A3) into (A2) and solving for E_1 gives then the result used in the text

$$E_1 = eV_1 - \alpha(\chi_1 - 1)L_1. \tag{A4}$$

APPENDIX II: CALCULATION OF SCATTERING BETWEEN VORTEX RINGS AND QUASIPARTICLES

A. General Formulation of the Problem

We should like to calculate the magnitude $\mathcal{F}$ of the frictional force on a vortex ring of radius R moving through liquid helium with a velocity v in the $\hat{z}$ direction. The discussion leading to Eq. (26) showed that, since the radius R is relatively large and the superfluid velocity at each ring element is v, the ring can be imagined straightened out so that the problem is reduced to the two-dimensional one of calculating the frictional force $\mathcal{F}'$ per unit length on a long straight vortex line (and associated superfluid) moving with a velocity v with respect to the quasiparticles of the fluid. Equivalently one can calculate this force $\mathcal{F}'$ by considering the vortex line stationary in the superfluid while the gas of quasiparticles moves with respect to this line with a mean velocity v in the $-\hat{z}$ direction. We shall adopt this last point of view in the following paragraphs and consider the geometrical situation illustrated in Fig. 10 where the $\hat{x}$ axis points along the vortex line. With the assumptions discussed in connection with Eq. (26), the total force on the vortex ring can then be computed by imagining the vortex line to be bent into a circle of radius R with its axis pointing in the $\hat{z}$ direction. Any components of $\mathcal{F}'$ in the $\hat{x}$ or $\hat{y}$ directions of Fig. 10 cannot contribute to the net force on the ring since they must cancel by symmetry; only the component in the $-\hat{z}$ direction contributes. Thus one can write

$$\mathcal{F} = (2\pi R)\mathcal{F}' = 2\pi R v(\mathcal{F}'/v). \tag{A5}$$

The last form reflects the expectation that $\mathcal{F}'$ is proportional to v so that $\mathcal{F}'/v$ is independent of v. Using the expression (6) for v, (A5) can then be written in the form (26) with

$$\alpha = \tfrac{1}{2}\kappa(\mathcal{F}'/v). \tag{A6}$$

The force $\mathcal{F}'$ is equal to the mean component of momentum in the $-\hat{z}$ direction transferred to unit length of the line per unit time by virtue of collisions with the quasiparticles of the fluid. Denote the momentum of a quasiparticle $\mathbf{p}$ and its energy (with respect to the superfluid at rest) by $\epsilon(p)$, where $p = |\mathbf{p}|$. We assume that the collision of a quasiparticle with a vortex line is elastic so that its energy is unchanged; then $p' = p$, where the prime denotes quantities after a collision.[47] We assume further that the momentum component parallel to the vortex line is unchanged as a result of collisions; thus $p_x' = p_x$, i.e., the angle θ specifying the direction of $\mathbf{p}$ with respect to the $\hat{x}$ axis, is unchanged. Denote the azimuthal angle of $\mathbf{p}$ about this axis by Φ before, and by $(\Phi+\varphi)$ after the collision. The line acquires in this kind of collision a component of momentum in the $-\hat{z}$ direction equal to $p_z' - p_z = p\sin\theta[\cos(\Phi+\varphi) - \cos\Phi]$. The probability of occurrence of scattering by an angle between φ and $\varphi + d\varphi$ is specified by the scattering cross section $\sigma(p;\varphi)d\varphi$ which gives the number of particles scattered into this angular range (per unit length in the $\hat{x}$ direction) per unit incident flux of quasiparticles incident on the line. This flux is given by $f(\mathbf{p})d^3\mathbf{p}(u\sin\theta)$, where $f(\mathbf{p})d^3\mathbf{p}$ denotes the mean number of quasiparticles per unit volume with momentum between $\mathbf{p}$ and $\mathbf{p}+d\mathbf{p}$ and where $u = |\partial\epsilon/\partial p|$ denotes the magnitude of the group velocity of such an excitation. The total force $\mathcal{F}'$ in the $-\hat{z}$ direction per unit length of line is then equal to

$$\mathcal{F}' = \int_{\mathbf{p}} [d^3\mathbf{p} f(\mathbf{p}) u\sin\theta] \times \int_{\varphi} p\sin\theta[\cos(\Phi+\varphi) - \cos\Phi]\sigma d\varphi, \tag{A7}$$

where the second integral is over all possible scattering angles φ and the first one over all possible momenta $\mathbf{p}$ of the incident quasiparticles.

The mean number $f(\mathbf{p})d^3\mathbf{p}$ of quasiparticles per unit volume in a thermal equilibrium situation where their mean velocity is $\mathbf{v}$ can readily be expressed in terms of the corresponding mean number $f_0(\epsilon)d^3\mathbf{p}$ in thermal equilibrium when their mean velocity vanishes (so that f_0 depends only on $|\mathbf{p}|$). Thus one has quite generally

$$f(\mathbf{p}) = f_0(\epsilon - \mathbf{v}\cdot\mathbf{p}) \approx f_0(\epsilon) - (\partial f_0/\partial\epsilon)\mathbf{v}\cdot\mathbf{p}, \tag{A8}$$

[46] Actual numerical integration yields 0.9 instead of 1 in (A3); this difference is negligible.

[47] In the case of rotons $p' \approx p = p_0$ to good approximation.

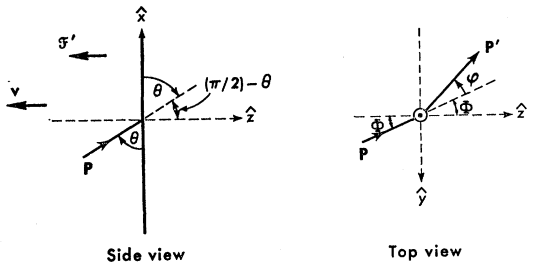

FIG. 10. Side and top views illustrating the scattering of a quasiparticle of momentum $\mathbf{p}$ by a vortex line.

where the last step uses the approximation that v is small. In our case $\mathbf{v}=-v\hat{z}$ so that $\mathbf{v}\cdot\mathbf{p}=-vp\sin\theta\cos\Phi$. Writing $d^3\mathbf{p}=p^2dp\sin\theta d\theta d\Phi$ and using (A8), integration of (A7) over all incident angles $0<\Phi<2\pi$ and $0<\theta<\pi$ gives then the result

$$\mathfrak{F}'=-\frac{3\pi^2}{8}v\int_0^\infty dp\frac{\partial f_0}{\partial\epsilon}up^4\sigma_0(p), \tag{A9}$$

where

$$\sigma_0(p)\equiv\int_0^{2\pi}(1-\cos\varphi)\sigma(p;\varphi)d\varphi \tag{A10}$$

is a total momentum-transfer cross section. Introducing the following average of this cross section over all momenta

$$\bar{\sigma}_0\equiv\int_0^\infty dp\frac{\partial f_0}{\partial\epsilon}up^4\sigma_0(p)\Big/\int_0^\infty dp\frac{\partial f_0}{\partial\epsilon}up^4 \tag{A11}$$

the result (A6) can then be written

$$\alpha=\frac{3\pi^2}{16}\kappa\bar{\sigma}_0\int_0^\infty dp\left(-\frac{\partial f_0}{\partial\epsilon}\right)up^4. \tag{A12}$$

B. Roton Scattering

Bose-Einstein statistics are applicable in the case of phonons and rotons so that

$$f_0(\epsilon)=h^{-3}(e^{\beta\epsilon}-1)^{-1}, \tag{A13}$$

where $\beta\equiv(kT)^{-1}$. For rotons the dispersion relation assumes the form

$$\epsilon=\Delta+(p-p_0)^2/2\mu. \tag{A14}$$

Hence $u=|\partial\epsilon/\partial p|=|p-p_0|/\mu$. Since $\beta\epsilon\gg1$, f_0 is only appreciable when p is close to p_0. Hence one can write $p\equiv p_0+\zeta$, use the fact that $|\zeta|\ll p_0$ wherever the factor $(\partial f_0/\partial\epsilon)$ in (A12) is appreciable, and extend the range of integration over ζ from $-\infty$ to $+\infty$ with negligible error. Using the subscript r for rotons, (A12) then becomes

$$\alpha_r=\frac{3\pi^2}{8}\frac{\kappa}{h^3}p_0^4e^{-\beta\Delta}\bar{\sigma}_{r0}. \tag{A15}$$

Here the effective cross section is given by (A11), the integrals being conveniently expressed in terms of the dimensionless variable $q\equiv(p-p_0)/(2\mu kT)^{1/2}$

$$\bar{\sigma}_{r0}=\int_{-\infty}^\infty dqe^{-q^2}|q|\sigma_{r0}(p_0+(2\mu kT)^{1/2}q). \tag{A16}$$

C. Phonon Scattering

The distribution (A13) is still applicable, but the dispersion relation is simply $\epsilon=cp$ where c is the velocity of sound. Thus $u=\partial\epsilon/\partial p=c$. Hence (A12) becomes, using the subscript p for phonons,

$$\alpha_p=\frac{\pi^6}{20}\frac{\kappa}{h^3}\left(\frac{kT}{c}\right)^4\bar{\sigma}_{p0}. \tag{A17}$$

Putting $q\equiv p(kT/c)^{-1}$, the effective cross section (A11) is here given by

$$\bar{\sigma}_{p0}=\frac{15}{4\pi^4}\int_0^\infty dqe^q(e^q-1)^{-2}q^4\sigma_{p0}\left(\frac{kT}{c}q\right). \tag{A18}$$

D. He^3 Scattering

The dispersion relation for a He^3 atom is simply $\epsilon=p^2/(2m^*)$, where m^* is its effective mass. Hence $u=p/m^*$. The He^3 impurity atoms obey Maxwell-Boltzmann statistics since their number n_3 per unit volume is quite small. Hence

$$f_0d^3\mathbf{p}=n_3(2\pi m^*kT)^{-3/2}e^{-\beta\epsilon}d^3\mathbf{p} \tag{A19}$$

which is properly normalized so that integration over all momenta yields n_3. Using the subscript 3 for He^3 atoms, the attenuation coefficient (A12) for scattering due to He^3 atoms becomes then

$$\alpha_3=\tfrac{3}{8}\kappa(2\pi m^*kT)^{1/2}n_3\bar{\sigma}_{30}. \tag{A20}$$

The effective cross section (A11) can here be written, putting $q\equiv p(2m^*kT)^{-1/2}$,

$$\bar{\sigma}_{30}=\int_0^\infty dqe^{-q^2}q^5\sigma_{30}((2m^*kT)^{1/2}q). \tag{A21}$$